CrossMark

Thermal analysis of the by-products of waste combustion

Michał Łach[1] · Janusz Mikuła[1] · Marek Hebda[1]

Abstract Every year, vast amounts of wastes are produced in households and in industrial facilities. Therefore, waste thermal treatment has become one of the most effective and popular methods of waste disposal and waste management. However, it inevitably leads to the creation of solid by-products, as ash and slag often containing substances which are toxic and harmful for environment. Hence, they must be further processed to be deprived of undesirable properties. In order to effectively bind or neutralize such materials, one should thoroughly know their properties. Unfortunately, they can vary greatly depending on the particular combusted material and combustion system. Yet, the detailed properties of the by-products of waste combustion may be thoroughly examined by means of combined methods of thermal analysis. The results of the research presented in this paper concern the possibility of determining the properties and detailed characteristics of waste combustion by-products by means of the combined techniques of thermal analysis. The examination was conducted on: dust from the boiler, bottom slag and ash, and solid waste from the exhaust gas cleaning. Test samples were obtained from one of the largest hazardous waste incineration plants in Poland. The investigated materials have undergone coupled thermal analysis (mass spectrometer connected with TG and DSC), which allowed for the detailed interpretation of the processes taking place during the examination of their thermal resistance. Moreover, morphology of the waste materials were analysed by SEM. Particle size distribution was determined by means of laser diffraction. Furthermore, content of harmful substances was examined.

Keywords Coupled technique · TG/DSC/QMS · Harmful substances · By-products of waste combustion

Introduction

Every year, vast amounts of waste are produced in households and in industrial facilities. All wastes are typically divided into municipal, hazardous and other. Because of the variety of origin wastes can have very different physical, chemical and mineralogical composition. The Europe 2020 strategy, particularly the initiative "Effective Use of Resources in Europe", unequivocally set the following goals: obtaining the resources by means of recycling and conducting research on innovative solutions able to reduce the degradation of the environment.

Thermal treatment is more and more often used to neutralize wastes [1] as it allows for energy recovery (e.g. by means of electricity generation) and for the reduction of the solid mass of original wastes by 70 % and their volume by up to 90 % [2]. The current methods of waste thermal treatment are very effective, but they generate significant amounts of undesirable by-products. In the case of municipal wastes incinerators, these are mostly slag and two kinds of ash (from mesh filters and from recovery boilers). In the case of hazardous waste incinerators, the wastes consist mostly of fly ash and slag [3]. It is estimated that from each tonne of wastes, 342 kg of solid wastes is generated (5 kg of ash, 300 kg of slag, 5 kg of fly ash, 20 kg of dust from extraction and 12 kg of various products from the exhaust gases cleaning system). All those by-products must be properly managed not to pose a threat to

✉ Marek Hebda
mhebda@pk.edu.pl

[1] Institute of Materials Engineering, Cracow University of Technology, ul. Warszawska 24, 31-155 Kraków, Poland

the environment. They are typically placed in landfills or recycled. Most developed countries have adopted their policies towards the reduction of the number of landfills and simultaneous development of new methods of waste recycling [4–6].

Slag has already found application in the construction industry whereas fly ash is very often considered hazardous waste because it contains heavy metals [7]. Extensive research is currently conducted on the recycling of slag and fly ash generated in municipal waste and hazardous waste incinerators (e.g. to use them as construction aggregate) [3]. Such wastes are also subjected to vitrification [8–11]. Owing to such treatment, one may reduce the volume of wastes, destroy all their organic components and embed heavy metal into amorphous structure. Wastes from incineration plants are more and more often neutralized by means of geopolymer matrix whose properties are very much suitable for it [12].

In the EU, fly ash from municipal waste incineration plants is classified as hazardous waste. Therefore, one must determine the specific hazardous components—first of all the contents of heavy metals, chlorides and sulphates— within the ash before the neutralization process takes place. Indeed, leaching tests have proved that heavy metals, chlorides and sulphates are released from fly ash from municipal waste incineration plants in such significant amounts that those wastes exceed the standards provided by the law and cannot be placed in ordinary landfills. It is also believed that without the initial treatment by means of washing, their neutralization cannot be economical [13].

However, the above-mentioned wastes can be economically neutralized by virtue of geopolymerization process, which is very often the best and the cheapest long-term waste management solution. In comparison with alternative technologies, geopolymerization has many advantages. It may be applied to manifold types of wastes. The obtained materials have good mechanical properties and may be used in the construction industry. Moreover, geopolymer materials are so resistant to environmental conditions that they may be used as an impermeable protective layer in landfills which separates the harmful wastes from the environment [14].

Due to the significant amounts of wastes and the fact that their composition varies, one must first determine their specific properties by virtue of advanced examination methods and on that basis apply the most appropriate neutralization technology. Thermal analysis is a very useful technique to identify the different kinds of fly ashes and

Table 1 Notation of samples, waste codes and waste descriptions

Notation of samples	Waste code	Waste description
1	190107*	Solid wastes from exhaust gases cleaning
2	190112	Bottom slag and ash
3	190115*	Boiler dust containing hazardous substances

According to the European Waste Catalogue, there are 15 types of wastes with code 1901—waste from incineration or pyrolysis of waste. Waste containing hazardous substances additionally is marked with *

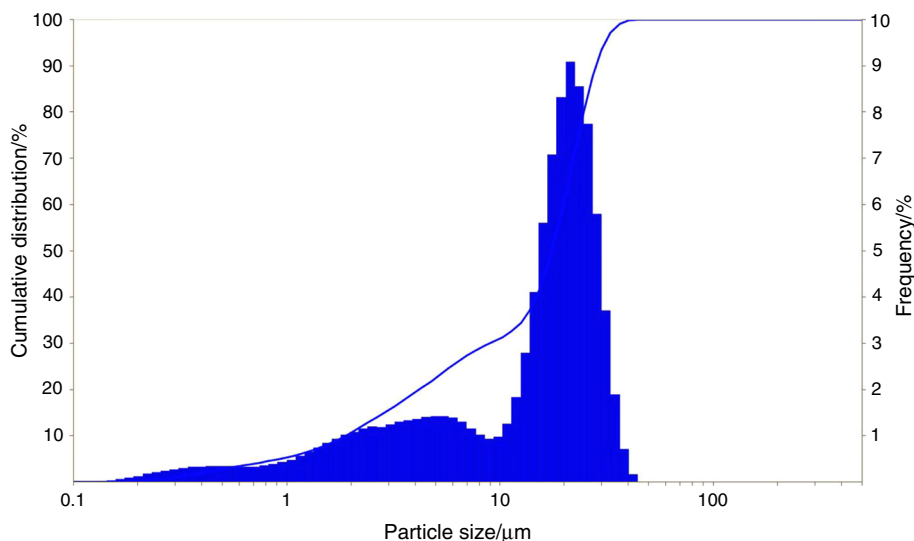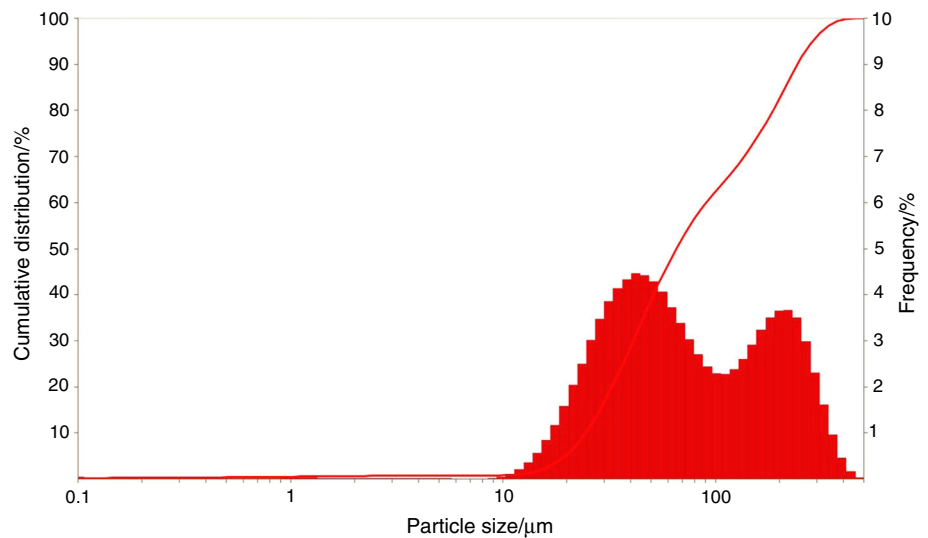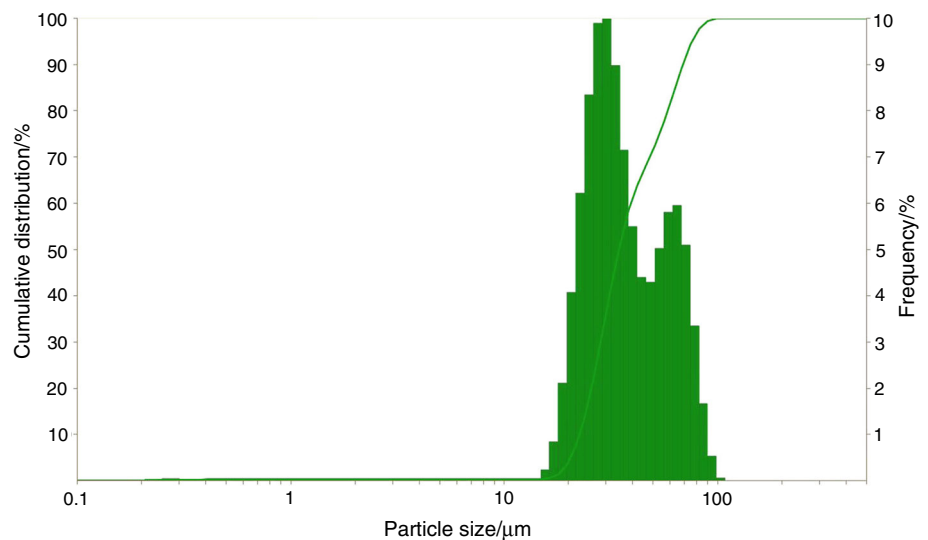**Fig. 1** Particle size distribution of the sample 1

Fig. 2 Particle size distribution of the sample 2

Fig. 3 Particle size distribution of the sample 3

Table 2 Particle size distribution of the analysed ashes

	Notation of samples		
	1	2	3
D10/μm	6.4 ± 3.4	25.6 ± 1.5	23.8 ± 1.8
Median D50/μm	19.6 ± 3.0	78.1 ± 17.9	36.8 ± 3.2
D90/μm	31.6 ± 4.6	286.2 ± 58.9	69.3 ± 0.8
Span/μm (D90-D10)/D50	1.0 ± 0.7	3.3 ± 0.1	1.2 ± 0.1
Mean/μm	22 ± 8.5	123.3 ± 26.0	42.2 ± 2.1
Mode/μm	25.2 ± 5.5	99.1 ± 79.9	32.6 ± 4.0

residues from waste incineration plants. These techniques are used for ash and other similar materials characterization since the 1980s. Recently, more frequently thermal analysis techniques are used to characterization materials based on fly ashes and residues from waste incineration plants [9–11, 15–18].

According to the results of the research elaborated in this paper, the coupled thermal analysis (mass spectrometer connected with TG and DSC) may allow for determining the characteristics of materials obtained through the waste thermal conversion. The research concerned three types of by-products of thermal neutralization: (1) boiler dust, (2) bottom slag and ash and (3) solid wastes from the exhaust gas cleaning, coming from one installation of the largest hazardous waste incineration plants in Poland.

The investigated materials have undergone coupled thermal analysis, which allowed for the detailed interpretation of

Fig. 4 Surface morphology of
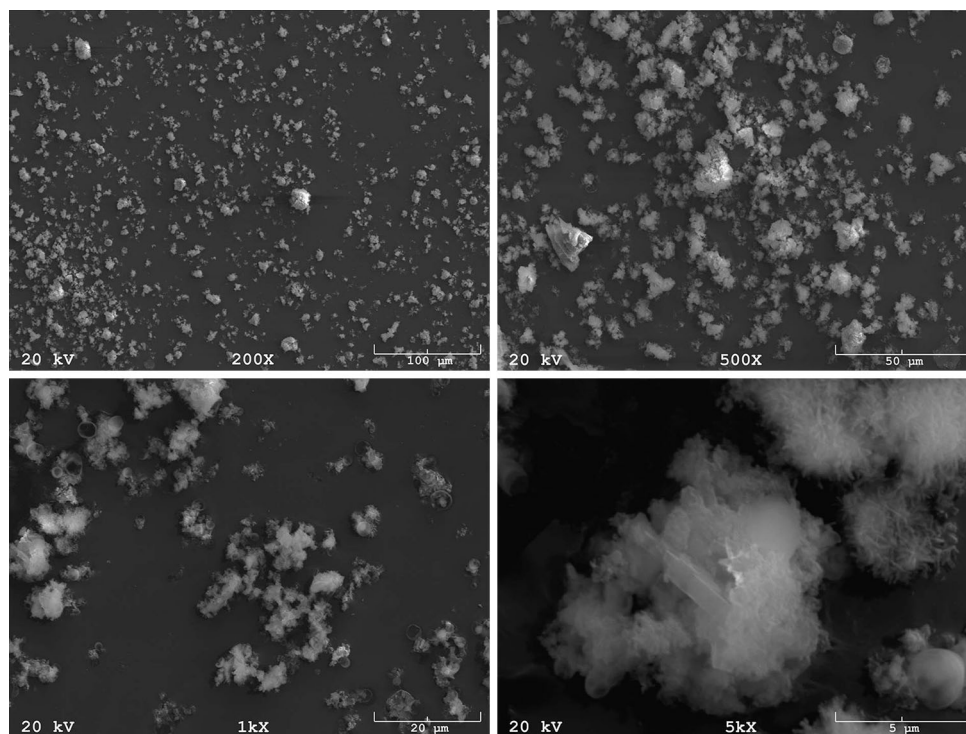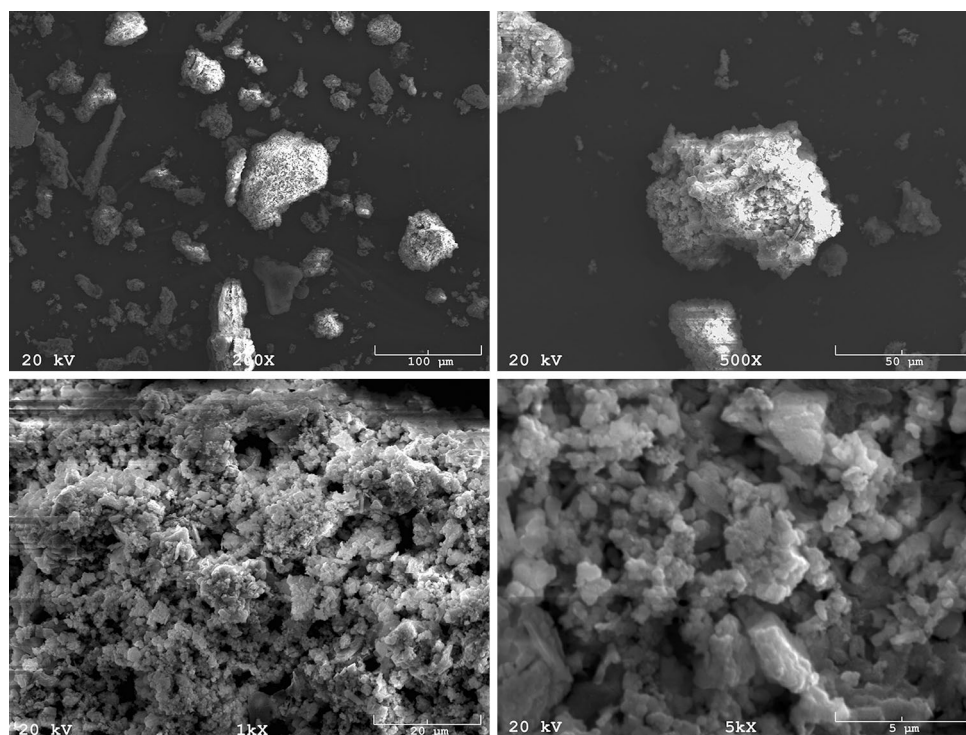the sample 1

Fig. 5 Surface morphology of
the sample 2

the processes taking place during the examination of their
thermal resistance. Moreover, morphology of the ash was
analysed with SEM. Particle size distribution was determined
with laser diffraction. Furthermore, the content of harmful
substances was examined.

Experimental

The examination covered the by-products of waste com-
bustion taken from three locations of the thermal conver-
sion system in one of the largest installations for hazardous

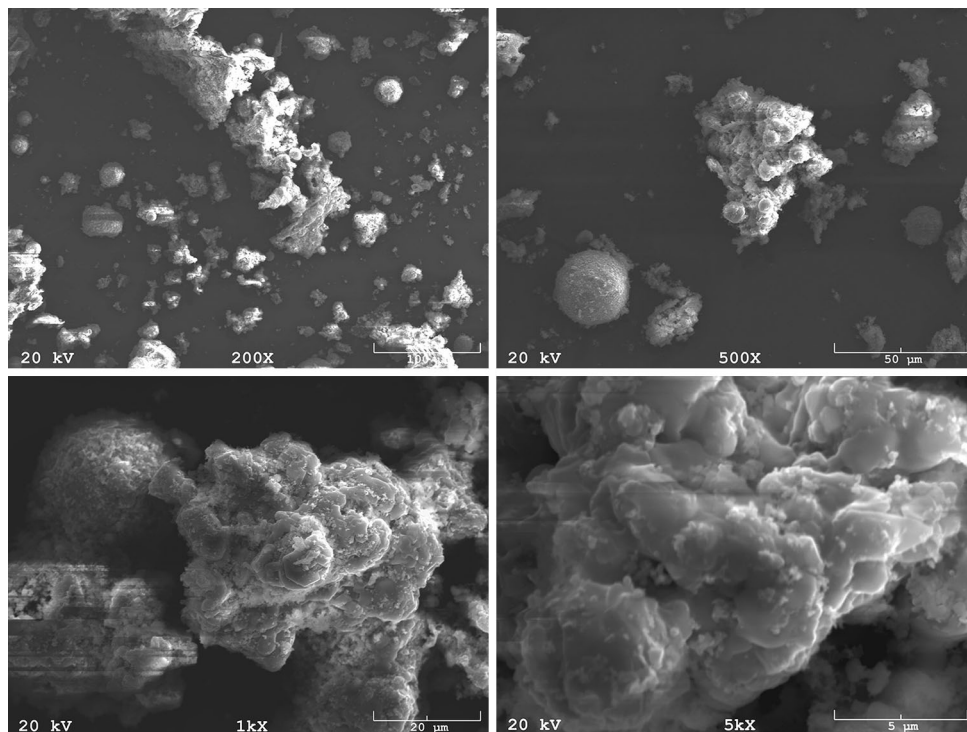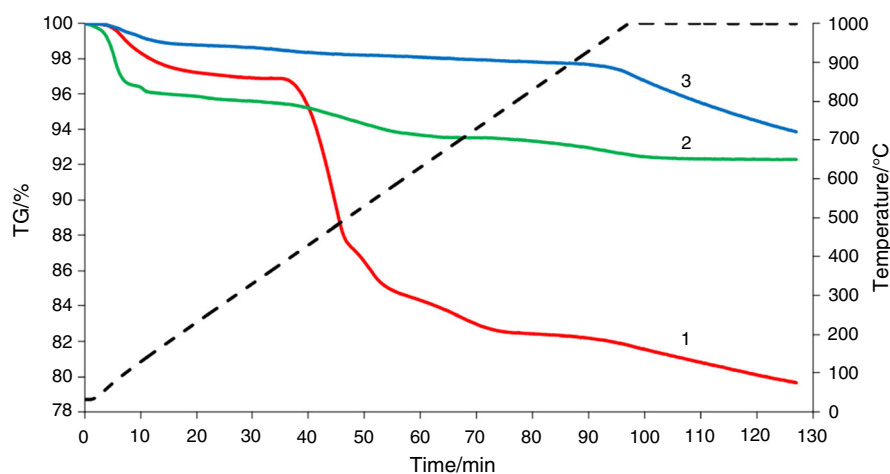**Fig. 6** Surface morphology of the sample 3

Fig. 7 Observed mass changes in the examined post-process wastes as a function of temperature (the *dotted line*) and time

waste incineration plants in Poland, with an efficiency up to 25,000,000 kg year^{-1}. The incineration plant used a counter-current rotary kiln with a cylindrical combustion chamber. The combustion temperature was in the range of 850–1000 °C, while the temperature in the afterburning chamber was between 1100 and 1300 °C. Gas cleaning was conducted through the use of systems (1) for reducing emissions of NOx by injection of urea to the cooling tower and (2) chemical neutralization of acid gas components as well as adsorption of heavy metals by injection of sodium bicarbonate together with the activated carbon into the exhaust stream. Moreover, wet chemical scrubber systems

were used to clean the exhaust streams. Samples without the use of selection processes were collected on different days, e.g. on 22 October 2013, 06 November 2013, 17 June 2014 and 13 March 2015. Metal leaching measurements showed no discrepancy between the results obtained for samples taken on different days; therefore, samples collected on 13 March 2015 were chosen for the investigation that is presented in this article. Table 1 presents sample labels, waste codes and waste descriptions.

Particle size distribution (using wet dispersions) was determined by means of laser diffraction (Fritsch Analysette 22 MicroTec plus model). Volume size distribution

Fig. 8 DTG curves of the examined post-process wastes as a function of temperature (the *dotted line*) and time
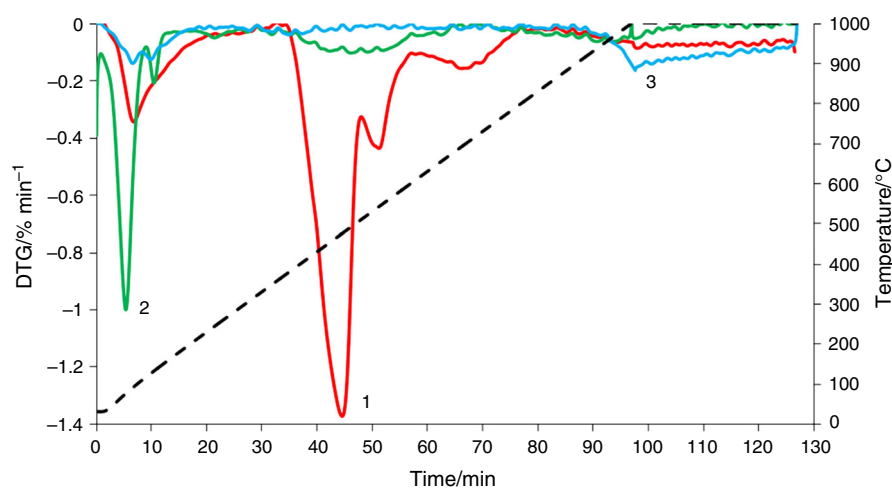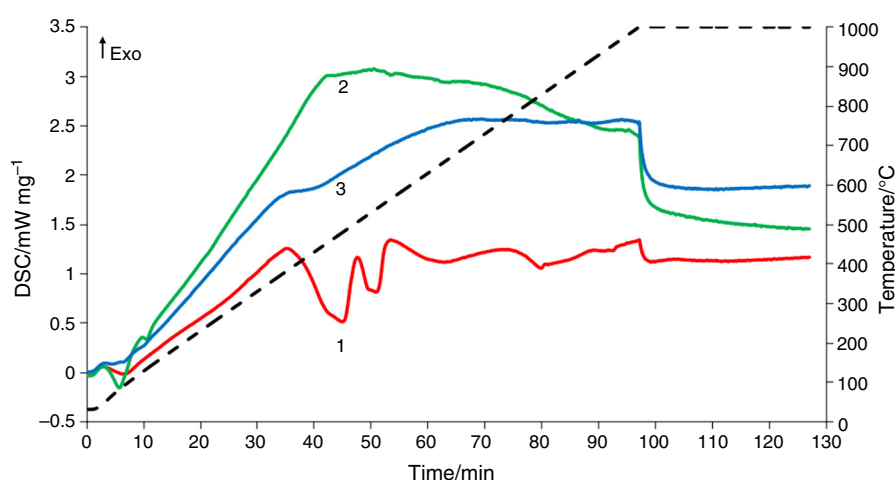

Fig. 9 DSC curves of the examined post-process wastes as a function of temperature (the *dotted line*) and time


was calculated automatically and expressed as D10, D50 (median) and D90. Five measurements were taken for each sample. The samples for the morphology examination were properly prepared using the scanning microscope JEOL JSM-820. Tiny amounts of ashes were dried to constant mass and then placed on the coal base in order to discharge samples. They were also covered with thin layer of gold with the JEOL JEE-4X vacuum evaporator.

Simultaneous thermogravimetry/differential scanning calorimetry (TG/DSC) was performed with an STA 409 CD (Netzsch) by virtue of advanced coupling TG/DSC with evolved gas analysis by quadruple mass spectrometry (QMS 403/5 SKIMMER). The apparatus was calibrated according to the procedure given in [19]. The temperature range was from 30 to 1000 °C and a heating rate of 10 °C min^{-1}. The holding time at the isothermal sintering temperature (at 1000 °C) was 30 min. The on-line gas analysis (distance between the sample and QMS was less than 20 mm) was studied by means of QMS with electron

ionization source. The spectrometer was operated in MID (multiple ion detection) mode. Air was used as a carrier gas at a flow rate of 80 mL min^{-1}. The QMS was checked with calcium oxalate monohydrate ($\geq$98 %, Fluka). The TG/QMS data were analysed with the Proteus software (ver. 5.2.0) by Netzsch. All the presented curves were corrected for baselines by performing additional experiments under the same conditions using empty crucibles. Three measurements were taken for each sample. Standard deviation of measurements did not exceed 0.5 %.

The content of dioxins was determined with gas chromatography coupled with mass spectrometry (GC–MS/MS) by the team of the Laboratory of Trace Analysis at the Institute of Inorganic Chemistry and Technology at the Cracow University of Technology. The examination was carried out according to the P/01/03 procedure imposed on 11 March 2010. The results were expressed as the upper limit of TEQ (toxic equivalency) according to the I-TEF (1988).

Fig. 10 Mass spectra obtained via MID mode of the sample 1 as a function of temperature (the *dotted line*) and time
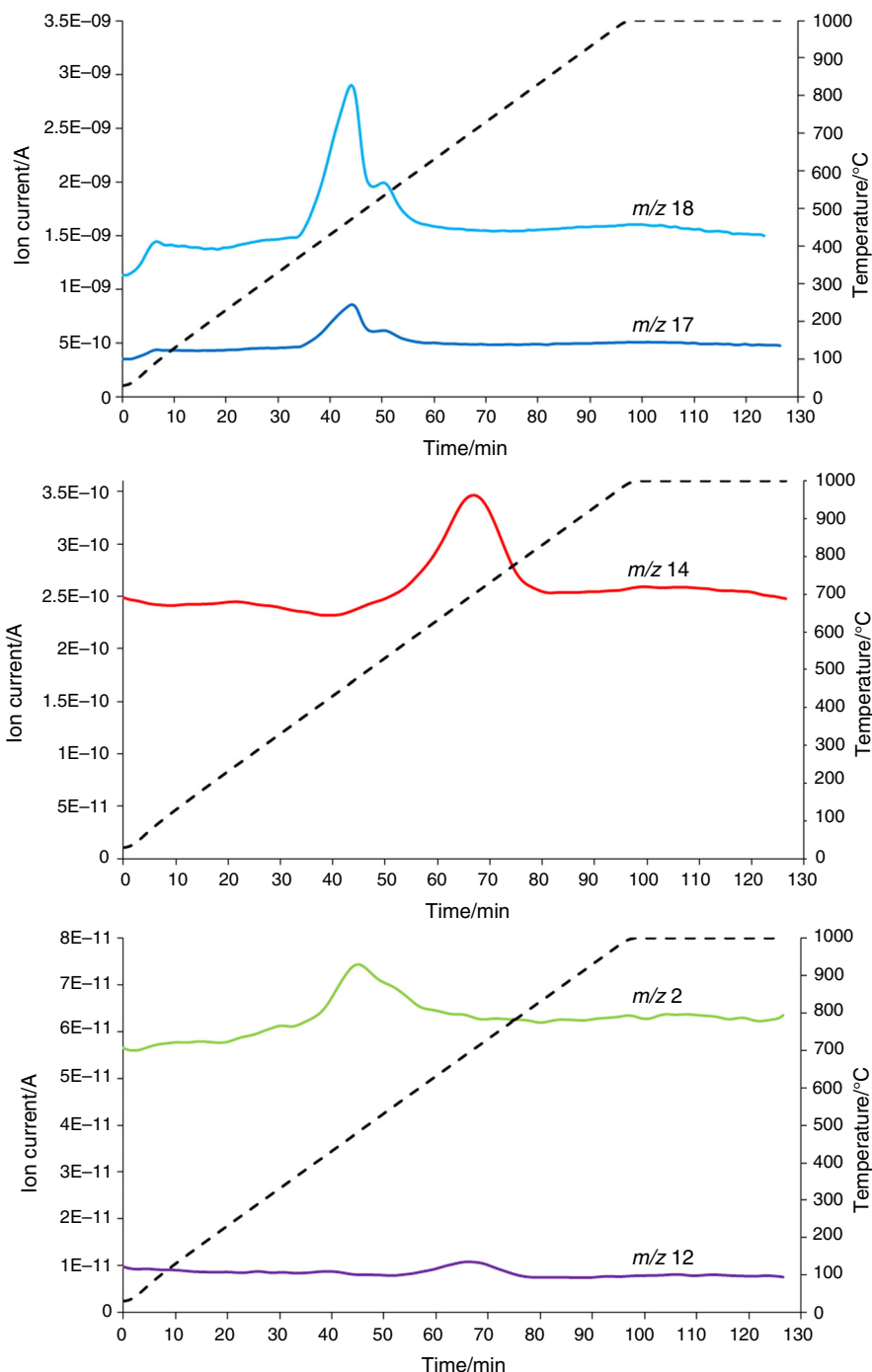
Results and discussion

Figures 1–3 and Table 2 present the size distribution of the products of thermal conversion of the examined samples. It was observed that the distribution was bimodal (with two well-visible extrema) in all the samples. The samples contained particles of various size, but in each of them one fraction, typical of that specific waste, was dominant.

According to the results, sample 1—the product of exhaust gases cleaning—contained the finest particles. Here, the amount of particles whose size was 2–10 μm was significant. The proof of it is the first extremum on the curve where the recorded maximum was 25.2 μm. Ten percent of the particles did not exceed 6.4 μm, and there were no particles larger than 45 μm.

On the other hand, sample 2 contained the largest particles of all. They were up to 400 μm, and it is worth

Table 3 Evolution of mass changes along with temperature ranges of analysed materials

TG changes		Notation of samples		
		1	2	3
1 step	Onset/°C	30.0	30.0	30.0
	Endset/°C	383.6	115.9	214.2
	Mass changes/%	−3.1	−3.5	−1.2
2 steps	Onset/°C	383.6	115.9	214.2
	Endset/°C	493.4	139.9	960.8
	Mass changes/%	−9.0	−0.4	−1.3
3 steps	Onset/°C	493.4	139.9	960.8
	Endset/°C	558.4	397.6	1000
	Mass changes/%	−2.6	−0.7	−3.7
4 steps	Onset/°C	558.4	397.6	–
	Endset/°C	766.1	722.1	–
	Mass changes/%	−2.8	−1.9	–
5 steps	Onset/°C	766.1	722.1	–
	Endset/°C	1000	1000	–
	Mass changes/%	−2.9	−1.2	–
Loss on ignition	%	−20.4	−7.7	−6.2

Table 5 Evolution of DSC changes along with temperature ranges of analysed materials

DSC changes		Notation of samples		
		1	2	3
1 effect endo (due to water)	Onset/°C	41.3	47.0	42.1
	Peak max/°C	91.1	80.7	89.3
	Endset/°C	123.7	101.1	131.5
2 effect endo	Onset/°C	393.5	125.2	336.2
	Peak max/°C	483.3	132.8	401.3
	Endset/°C	504.5	145.3	467.7
3 effect	Onset/°C	504.5	407.1	–
	Peak max/°C	542.5	425.0	–
	Endset/°C	555.6	–	–
4 effect exo	Onset/°C	555.6	–	–
	Peak max/°C	641.8	–	–
	Endset/°C	777.1	–	–
5 effect exo	Onset/°C	777.1	–	–
	Peak max/°C	824.8	–	–
	Endset/°C	895.0	–	–

Table 4 Values of peak extremum on DTG curves for all the examined samples

Temperature °C of registration	Notation of samples		
	1	2	3
1 extremum	92.9	76.1	108.3
2 extremum	475.5	132.7	Lack of a clear effect
3 extremum	542.3	243.6	In isotherm
4 extremum	690.9	491.1	–
5 extremum	∼1000	937.0	–

Table 6 Moisture measurement of the raw materials

Notation of samples	Moisture of the raw material/%
1	2.04 ± 0.03
2	7.58 ± 0.13
3	1.03 ± 0.05

polyhedral or oval crystalline precipitates. On the other hand, particles in the sample 2 had a very different morphology because they consisted of amorphous and crystalline phases. Their surface was well developed and resembled a set of the enormous amount of very fine polyhedral crystals (Fig. 5). The observed surface morphology was independent on the particle size. As for the sample 3 (Fig. 6), it was a mixture of polyhedral and spheroid particles (the former were dominant). The larger particles were in most cases conglomerates with well-visible spheroid areas on the developed surface. However, the surface of those particles was less developed in comparison with the particles in sample 2. The microscopic images are fully consistent with the results of the laser measurement of the size of powder particles.

Figure 7 shows the recorded mass changes of the examined post-process wastes as a function of temperature and time. The greatest mass loss was observed in the case of sample 1. That process ran in several stages, and the whole loss on ignition—widely believed to be one of the best indicators of the incineration accuracy [20]—was 20.4 %. According to the DTG curves (Fig. 8) and the

noticing that no particle was smaller than 10 μm. The first maximum on the curve was observed at 42.6 μm and the second at 220 μm. Sample 2 had the widest span of particles (span = 3.3).

In the case of sample 3, the values of particle size distribution were intermediate between those observed for the samples 1 and 2 (the best proof of it is the mean values presented in Table 2). The maximum of the curve was at 29.8 μm, and the next peak was at 65 μm. Sample 3 contained the particles whose size was 16–120 μm. The span of the curve was similar to the sample 1.

Figures 4–6 present the surface morphology of the examined samples of the ash. It was observed that the morphology of most common fraction of particles in the sample 1 was jagged/feathery and that larger particles were probably conglomerates of the smaller ones and included

Fig. 11 Mass spectra obtained via MID mode of the sample 2 as a function of temperature (the *dotted line*) and time
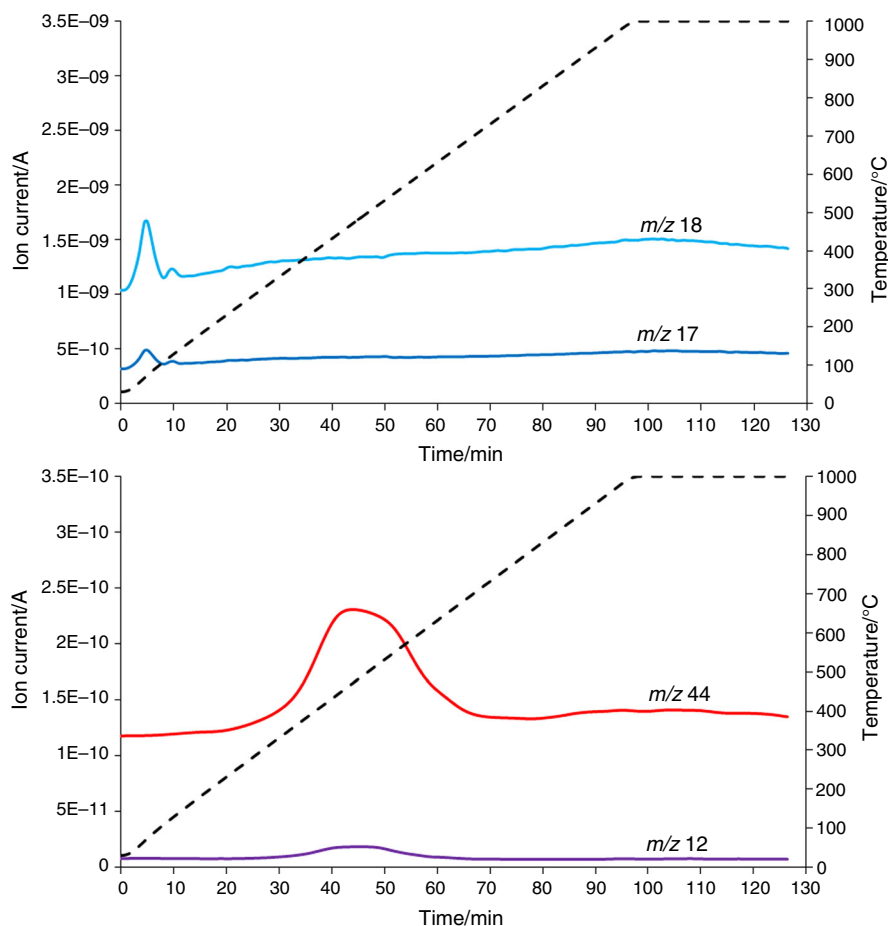
determined peak extrema (Table 4), the most dynamic mass loss was at approx. 100 and 500 °C. The former was approx. 3 % and resulted from the evaporation of moisture and water absorbed by the sample, which is reflected in the endothermic effect on the DSC curve (Table 5; Fig. 9) and in the increased amount of released gas products *m/z* 17 and *m/z* 18 (Fig. 10). The second mass loss, which was the most significant (approx. 9 %, Table 3), as well as the third one also pertained to water release. Most probably, it stemmed either from the chemical reactions whose product is water, or from the decomposition of crystallization water present in the jagged/feathery structural framework of the particles. The intensity of the signals measured by means of mass spectrometry was fully consistent with the course of the TG curve. It was also observed that at approx. 100 and 500 °C, *m/z* 2 signal was stronger, which may resulted from the decomposition of bonds in water molecules or other hydrogen bonds in the examined ash. The fourth and fifth mass losses took place at the higher temperature range (above 558 °C), amounted to approx. 3 % each. They were related to the exothermic effects visible on the DSC curve and to the release of gas products *m/z* 44 and *m/z* 12. On that basis, one may conclude that at

this temperature range, carbon/organic remains in the sample 1 are incinerated.

According to the thorough thermal analysis, sample 2 had the most significant mass loss at the temperature range up to 140 °C. Here, the mass loss was a two-stage process (Figs. 7, 8; Tables 3, 4) whose first step amounted to 3.5 % and the second only to 0.4 % sample mass (also according the DSC and MID curves the former effect is much stronger than the latter Fig. 9, 11). The release of water in such low temperatures was so easy because the size of ash particles in that sample was larger than in other ones and they had crystalline and well-developed structure. Besides, the measurement of moisture of the raw materials (Table 6) proved that the sample 2 contained significant amount of adsorbed water (it was almost three times larger in comparison with the sample 1 and seven times larger in comparison with the sample 3). In the case of sample 2, above 400 °C thermal decomposition of organic remains took place reflected by, e.g., (1) significant increase of the amount of released gas products *m/z* 12 (C) and *m/z* 44 (CO_2) (see Fig. 11); (2) further two-step mass loss amounting to approx. 3.1 % sample mass (Figs. 7, 8); and (3) observed exothermic effect on the DSC curve (Fig. 9).

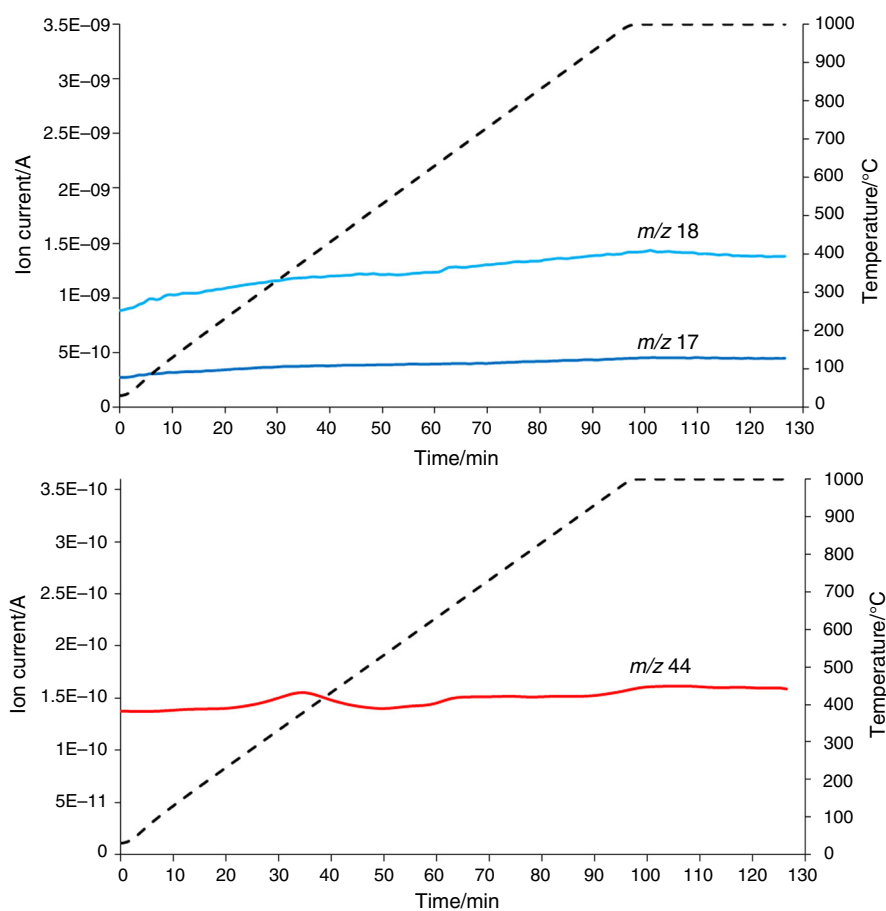Fig. 12 Mass spectra obtained via MID mode of the sample 3 as a function of temperature (the *dotted line*) and time

Table 7 Total amount of dioxins in the samples

Notation of samples	Total amount of dioxins (I-PCDD/F-TEQ)/(ng g^{-1})
1	1.30 ± 0.32
2	0.30 ± 0.08
3	1.40 ± 0.36

Sample 3 was the least vulnerable to changes when subjected to thermal analysis. Its loss on ignition was 6.2 % (Table 3). It is worth noticing that mass loss became significant only up to 960 °C and was accompanied by the release of m/z 44. Contrary to the samples 1 and 2, sample 3 contained hardly any water particles (Fig. 12). The results of the thermal analysis are consistent with the moisture measurement of the raw materials (Table 6)—according to them, moisture of the sample 3 was approx. 1 %.

Table 7 presents the results of the measurement of dioxin content in the post-process wastes. One should remember that the by-products of waste thermal treatment contain a significant amount of dioxins which are strongly bound to ash and hard to flush. They also barely decompose

in ash, and their neutralization (mainly via dichlorination) is costly. According to the examination, the least amount of dioxins was observed in sample 2 (which had the largest particles of well-developed surface, and which adsorbed the largest amount of adsorbed water). The concentrations of dioxins in sample 1 and 3 were similar to each other and four times larger than in sample 2. The results are consistent with the observations by other researchers according to which bottom ash and slag usually contains a low amount of dioxins [21].

Conclusions

The examination concerned three various post-process wastes from the same commercial thermal waste incineration plants. According to the results, each of the examined wastes has some specific physical–chemical characteristics (particle size, moisture, dioxins content and thermal stability). Sample 2 (bottom slag and ash) contained the largest particles and the least amount of adsorbed dioxins; as a raw material, it had the highest level of moisture. Samples 1 and 3 contained much finer particles and much higher concentration of dioxins. By means of the TG/DSC/QMS

coupled analysis, it was proved that thermal stability of the samples strictly depends on their type. Sample 1 (solid waste from exhaust gases cleaning) stood for the most significant changes on TG/DSC curves and in released gas products, whereas in the case of sample 3 (boiler dust), TG/DSC effects were the least intensive and took place at the very high temperatures. The obtained results demonstrate the usefulness of the coupled thermal analysis in the identification of the type of by-products from waste thermal incineration.

References

1. Liu A, Ren F, Lin WY, Wang JY. A review of municipal solid waste environmental standards with a focus on incinerator residues. Int J Sustain Built Environ. 2015;4(2):165–88.
2. Lam ChHK, Ip AWM, Barford IP, McKay G. Use of incineration MSW Ash: a review. Sustainability. 2010;2:1943–68.
3. Kępys W. Próba odzysku popiołów lotnych i żużli z instalacji termicznego przekształcania odpadów jako kruszywa sztucznego. Gospodarka Surowcami Mineralnymi. 2008;24:149–56.
4. Johannesses KM. The regulation of municipal waste incineration Ash: a legal review and update. J Hazard Mater. 1996;47(1–3):383–93.
5. Grela A, Hebda M, Łach M, Mikuła J. Thermal behavior and physical characteristics of synthetic zeolite from CFB-coal fly Ash. Microporous Mesoporous Mater. 2016;220:155–62.
6. Cioablă AE, Pop N, Calinoiu DG, Trif-Tordai G. An experimental approach to the chemical properties and the ash melting behavior in agricultural biomass. J Therm Anal Calorim. 2015;121(1):421–7.
7. Mokrosz W. Ekologiczne aspekty oczyszczania spalin ze spalarni odpadów komunalnych i przemysłowych. In: Proceedings of POL-EMIS; 2010. p. 263–72.
8. Haiying Z, Youcai Z, Jingyu Q. Measurement of composition variation of municipal solid waste incineration (MSWI) fly Ash during thermal treatment. Key Eng Mater. 2011;460–461:90–5.
9. Ciecinska M, Stoch P, Stoch A. Thermal properties of vitrified llw hospital waste incineration ash. J Therm Anal Calorim. 2014;116:35–9.
10. Yuan-yuan L, Jia-jia W, Xing L, Li-ao W, Shan Z, Wei Y. Microstructures and thermal properties of municipal solid waste incineration fly ash. J Cent South Univ. 2012;19:855–62.
11. Haiying Z, Youcai Z, Jingyu Q. Thermal characterization of fly ash from one municipal solid waste incinerator (MSWI) in Shanghai. Process Saf Environ Prot. 2010;88:269–75.
12. Galiano YL, Pereira CF, Vale J. Stabilization/solidification of a municipal solid waste incineration residue using fly Ash-based geopolymer. J Hazard Mater. 2011;185:373–81.
13. Ferone C, Colangelo F, Messina F, Santoro L, Cioffi R. Recycling of Pre-washed muncipal solid waste incinerator fly Ash in the manufacturing of low temperature setting geopolymer materials. Materials. 2013;6:3420–37.
14. Jaarsveld JGS, Deventer JSJ. The potential use of geopolymeric materials to immobilize toxic metals: part I. Theory and applications. Miner Eng. 1996;10(7):659–69.
15. Chandler AJ, van del Sloot HA HA, Vehlow J. Municipal solid waste incinerator residues. New York: The International Ash Working Group Elsevier; 1997.
16. Pacewska B, Wilinska I. Comparative investigations of influence of chemical admixtures on pozzolanic and hydraulic activities of fly ash with the use of thermal analysis and infrared spectroscopy. J Therm Anal Calorim. 2015;120:119–27.
17. Grela A, Łach M, Mikuła J, Hebda M. Thermal analysis of the products of alkali activation of fly ash from CFB boilers. J Therm Anal Calorim. doi:10.1007/s10973-016-5257-5.
18. Majchrzak-Kucęba I. Thermogravimetry applied to characterization of fly ash-based MCM-41 mesoporous materials. J Therm Anal Calorim. 2012;107:911–21.
19. Hebda M, Laska M, Szechyńska-Hebda M. Application of a device used for observation of controlled thermal processes in a furnace. J Therm Anal Calorim. 2013;114:1099–109.
20. Rocca S, van Zomeren A, Costa G, Dijkstra JJ, Comens RNJ, Lombardi F. Mechanisms contributing to the thermal analysis of waste incineration bottom ash and quantification of different carbon species. Waste Manag. 2013;33(2):373–81.
21. Pająk T. Dioksyny w procesie spalania odpadów komunalnych—zagrożenia, normy, aktualna sytuacja, przeciwdziałanie. Roczniki PZH. 1996;47:105–19.